Neuron, Vol. 20, 69–81, January, 1998, Copyright ©1998 by Cell Press

# Mice Deficient in $G_{olf}$ Are Anosmic

**Leonardo Belluscio,* Geoffrey H. Gold,† Adrianna Nemes,* and Richard Axel*‡**
*Department of Biochemistry and Molecular Biophysics
and Howard Hughes Medical Institute
College of Physicians and Surgeons
Columbia University
New York, New York 10032
†Monell Chemical Senses Center
Philadelphia, Pennsylvania 19104

## Summary

**We have used gene targeting to examine the role of the $G\alpha$ subunit, $G_{olf}$, in olfactory signal transduction. Mice homozygous for a null mutation in $G_{olf}$ show a striking reduction in the electrophysiological response of primary olfactory sensory neurons to a wide variety of odors. Despite this profound diminution in response to odors, the topographic map of primary sensory projections to the olfactory bulb remains unaltered in *$G_{olf}$* mutants. Greater than 75% of the *$G_{olf}$* mutant mice are unable to nurse and die within 2 days after birth. Rare surviving homozygotes mate and are fertile, but mutant females exhibit inadequate maternal behaviors. Surviving homozygous mutant mice also exhibit hyperactive behaviors. These behavioral phenotypes, taken together with the patterns of $G_{olf}$ expression, suggest that $G_{olf}$ is required for olfactory signal transduction and may also function as an essential signaling molecule more centrally in the brain.**

## Introduction

Sensory neurons respond to environmental stimuli and transmit these signals to the brain, where they are processed to allow for the discrimination of complex sensory information. The delineation of the peripheral mechanisms by which environmental stimuli are transduced into neural information can provide insight into the logic of sensory processing. Olfaction is the primary sensory modality by which many organisms communicate with their environment. The initial events in the detection of odors result from the association of odorous ligands with specific receptors on the cilia of olfactory neurons. The cilia are not only the site of odor binding but are also the site of signal transduction, such that odor recognition is translated into alterations in the membrane potential of olfactory sensory neurons. In vertebrates, odor binding results in an inwardly depolarizing current that ultimately triggers action potentials that travel along the sensory axon to the olfactory bulb (Kurahashi, 1989; Firestein and Werblin, 1989; Lowe and Gold, 1991). In this manner, odor binding in the periphery is translated into neural information in the brain.

How is odor binding translated into alterations in membrane potential in the olfactory cilia? In vertebrates, many odors elicit an increase in the intracellular second messenger cAMP, presumably as a consequence of the interaction of odorous ligands with putative seven transmembrane domain receptors that reside on the ciliary membranes (Pace et al., 1985; Sklar et al., 1986; Breer et al., 1990). In rodents, these receptors are encoded by a family of ~1000 distinct receptor genes (Buck and Axel, 1991; Levy et al., 1991; Parmentier et al., 1992; Ben-Arie et al., 1994), such that a given neuron expresses only one receptor (Buck, 1992; Chess et al., 1994; C. Dulac, R.A., unpublished data). Receptor occupancy is thought to activate a $G\alpha_s$ homolog, $G_{olf}$, expressed at high levels in olfactory cilia (Jones and Reed, 1989). Activated $G_{olf}$ is thought to stimulate the membrane-bound adenylate cyclase type III (Bakalyar and Reed, 1990). Elevations in cAMP then locally activate a cyclic nucleotide–gated (CNG) cation channel present in ciliary membranes, providing a mechanism for rapid electrical signaling (Nakamura and Gold, 1987; Kurahashi, 1989; Firestein et al., 1991; Frings and Lindemann, 1991; Lowe and Gold, 1993a). In this manner, exposure of sensory neurons to odors results in the generation of transient depolarizing currents that are then transmitted to the brain. Recent gene targeting experiments reveal an obligate requirement for the CNG channel (Brunet et al., 1996), but the role of $G_{olf}$ in olfactory signal transduction has not been experimentally examined. Olfactory sensory neurons express at least two $G\alpha_s$ homologs, $G_s$ and $G_{olf}$, each capable of activating adenylate cyclase (Jones and Reed, 1987, 1989). Although $G_{olf}$ is far more abundant than $G_s$ in the adult olfactory epithelium, either molecule could contribute to odor-evoked signaling (Jones et al., 1990).

Discrimination among odors then requires that the brain determine which of the numerous receptors have been activated by a given olfactory stimulus. Since individual olfactory neurons express only one of the 1000 receptor genes, the problem of determining which receptors have been activated can be reduced to a problem of distinguishing which neurons have been activated. Recent molecular and genetic experiments indicate that neurons expressing a given receptor, and therefore responsive to a given odor, project with precision to only two of 1800 glomeruli in the mouse olfactory bulb (Ressler et al., 1994a; Vassar et al., 1994; Mombaerts et al., 1996). Since the positions of individual glomeruli are topographically fixed in all individuals in a species, the bulb maintains a two-dimensional map of receptor activation such that the quality of an olfactory stimulus is encoded by the spatially defined patterns of glomerular activity in the olfactory bulb (Stewart et al., 1979; Lancet et al., 1982; Kauer et al., 1987; Imamura et al., 1992; Mori et al., 1992; Katoh et al., 1993; Friedrich and Korsching, 1997; Joerges et al., 1997).

In this study, we have used gene targeting to examine the role of the $G\alpha$ subunit $G_{olf}$ in olfactory sensory transduction. Mice homozygous for a null mutation in *$G_{olf}$* show a striking reduction in the electrophysiological response of the primary olfactory sensory neurons to a

‡To whom correspondence should be addressed.

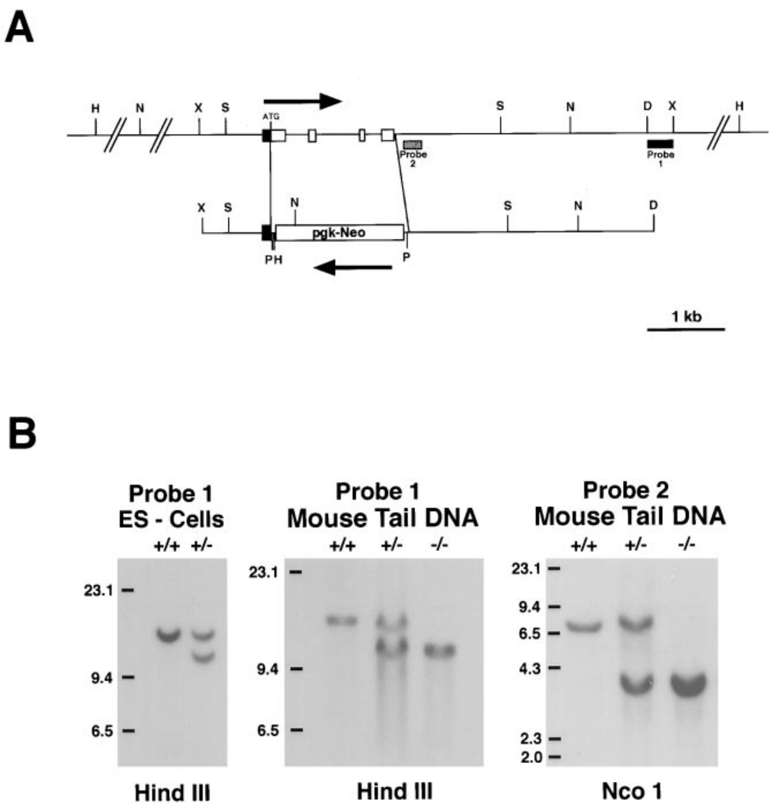


Figure 1. Targeted Disruption of the $G_{olf}$ Gene

(A) Schematic representation of the $G_{olf}$ targeting strategy. Homologous recombination between the wild-type $G_{olf}$ gene (top) and the targeting vector (bottom) results in the replacement of a 1.65 kb region of the $G_{olf}$ gene containing the first four exons with a 1.7 kb *pgk-neo* cassette. The proposed translational start site is marked by ATG. The exon structure is based on sequence homology with the rat and mouse *Golf* genes. Coding exons are shown as white boxes and the proposed 5′-nontranslated region is shown in black. The arrows define transcriptional orientation. H, HindIII; N, NcoI; D, NdeI; P, PacI; S, SacI.

(B) Southern blot analysis.

(Left) Wild-type (+/+) ES-cell DNA and DNA from a homologous recombinant (+/−) digested with HindIII and hybridized with Probe 1. The new 10 kb band in +/− cells reflects integration of the *neo*$^r$ gene at the $G_{olf}$ locus.

(Center) Tail DNA from littermates from a cross between F1 $G_{olf}$ heterozygotes was digested with HindIII and hybridized with Probe 1.

(Right) Tail DNA from an F1 cross-digested with NcoI and hybridized with Probe 2.

wide variety of odors. Moreover, mutant mice fail to feed, and most die shortly after birth. Despite the profound diminution in the electrophysiological response to odors, the topographic map of sensory projections is unaltered in $G_{olf}$ mutant animals. We also note that rare surviving homozygous mutants exhibit hyperactive locomotor behavior. These data demonstrate that $G_{olf}$ is not only required in olfactory sensory transduction but may function in neurons in the central nervous system (CNS).

## Results

### The Phenotype of $G_{olf}$-Deficient Mice

The mouse $G_{olf}$ gene shares 80% amino acid identity with the mouse gene encoding $G_s$. $G_s$ is encoded by 12 exons, and mutational analysis has demonstrated that the first four exons play a critical role in coordinating nucleotide binding, GTPase activity, and the interaction with effector enzymes (Masters et al., 1986, 1990; Miller et al., 1988; Conklin et al., 1996). Deletion of the region of the $G_{olf}$ gene containing these four exons should therefore result in a null allele. Homologous recombination was therefore performed with a targeting vector in which the first four exons of the $G_{olf}$ gene are replaced with the neomycin-resistance gene (*neo*$^r$) such that the *neo*$^r$ gene is transcribed in an orientation opposite that of $G_{olf}$ (Figure 1A). Southern blot analysis identified only one homologous recombinant in 300 *neo*$^r$ colonies obtained with the $G_{olf}$ targeting vector. A single targeted ES colony was expanded and used to generate several chimeric mice, which transmitted the mutation through the germline, permitting the generation of mice with a homozygous deficiency in the $G_{olf}$ gene (Figure 1B).

$G_{olf}$ homozygotes fail to thrive. At birth, the offspring from crosses between F1 heterozygotes were grossly indistinguishable. However, 2 days after birth, >75% of the $G_{olf}$ homozygotes died without milk in their stomachs, presumably as a consequence of the inability to suckle. About 1%–5% of the homozygous mutant mice ultimately begin to feed, but by 1 week these homozygotes show a 30% reduction in body weight and remain at a competitive disadvantage for feeding when compared with their heterozygous and wild-type littermates. Trimming the litter enhances the survival of homozygous mutant animals (see Experimental Procedures). At 3 weeks, when wild-type and heterozygous animals wean from the mother, homozygous mutants continue to nurse. If nursing persists, ∼5% of the homozygous mutant animals will survive to sexual maturity. Preliminary studies reveal that surviving male and female homozygotes mate and are fertile. However, all pups born to homozygous $G_{olf}$ mutant females die due to inadequate maternal behavior. Mutant mothers fail to nest or crouch over their pups in a typical nursing manner and neither collect nor retrieve them when they are scattered. This behavior has been observed for four litters from three different mothers. As a consequence of these defects in maternal behavior, all pups die without milk in their stomachs by postnatal day 2 (P2). Nursing and mothering behavior is mediated, at least in part, by the main olfactory system, suggesting that olfaction is impaired in $G_{olf}$ mutant mice (Teicher et al., 1980; Levy et al., 1991; Calamandrei et al., 1992; Mayer and Rosenblatt, 1993; Coppola et al., 1994; Romeyer et al., 1994; Griffith and Williams, 1996; Brunet at al., 1996). At ∼5 weeks of age, surviving homozygous mutant mice begin to exhibit

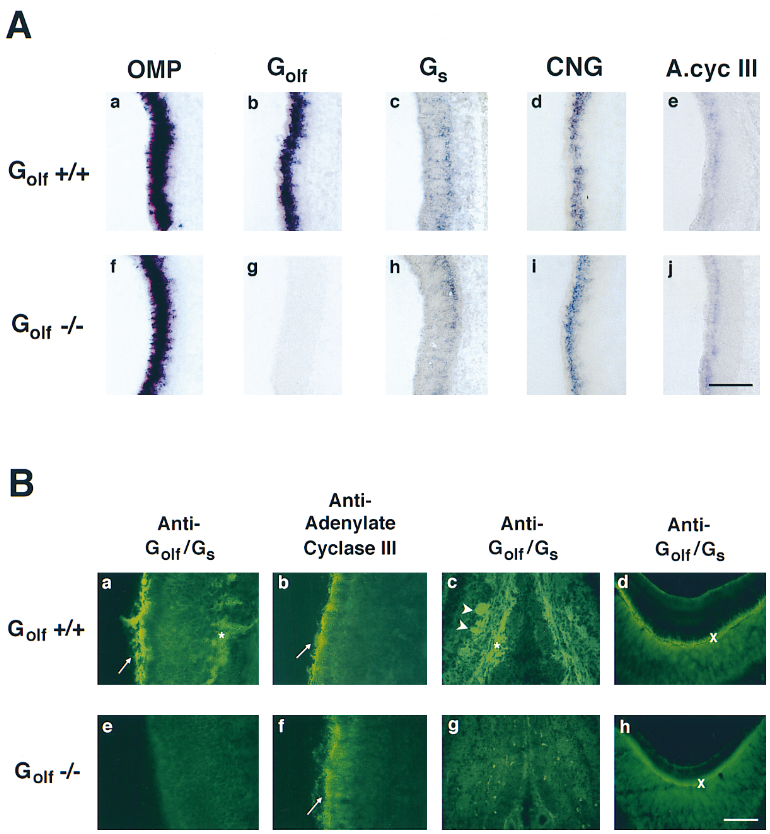


Figure 2. Patterns of Gene Expression in Wild-Type and $G_{olf}$ Mutant Mice

(A) Expression of RNA encoding olfactory signal transduction components in wild-type and $G_{olf}$ mutant mice. In situ hybridization was performed on 15 μm coronal sections of mouse olfactory epithelium from 5-day-old mice using digoxigenin–labeled anti-sense RNA probes. All panels used alkaline phosphatase–conjugated anti-digoxigenin antibody to visualize positive signals shown in dark purple.

(a–e) Adjacent sections derived from wild-type mice.

(f–j) Ajacent sections derived from $G_{olf}$ mutant animals. Probes used: ([a] and [f]) OMP; ([b] and [g]) $G_{olf}$; ([c] and [d]) $G_s$; ([d] and [i]) CNG, α-subunit of olfactory cyclic nucleotide–gated channel; and ([e] and [j]) adenylate cyclase type III. Scale bar, 100 μm.

(B) Immunolocalization of $G_{olf}$ and adenylate cyclase III in wild-type and $G_{olf}$ mutant mice. Specific primary antibody was applied to 15 μm coronal head sections through the main olfactory epithelium olfactory bulb and upper jaw. The signal was visualized using Cy2-conjugated secondary antibody.

(a and e) Antibody to $G_{olf}/G_s$ applied to olfactory epithelium.

(b and f) Antibody to adenylate cyclase applied to olfactory epithelium.

(c and g) Antibody to $G_{olf}/G_s$ applied to olfactory bulb.

(d and h) Antibody to $G_{olf}/G_s$ applied to jaw shows a developing tooth.

Arrows denote olfactory cilia; arrowheads denote glomeruli; asterisk denotes axon bundles in the olfactory epithelium and the outer nerve layer of the bulb; X denotes odontoblast layer of the developing tooth. Scale bar, 50 μm for (a), (b), (d), (e), (f), and (h); 150 μm for (c) and (g).

hyperactive locomotor behaviors (see below and Figure 7). These behavioral phenotypes suggest that $G_{olf}$ may be an essential signal transduction component not only in olfactory sensory neurons but more centrally in the brain as well.

## Expression of Olfactory Components in Wild-Type and Mutant Mice

In initial experiments, we characterized the molecular anatomy and electrophysiology of the olfactory sensory epithelium. We have used in situ hybridization to $G_{olf}$ RNA along with immunocytochemistry to document the absence of $G_{olf}$ in mutant animals (Figure 2). In wild-type animals, in situ hybridization with digoxigenin-labeled $G_{olf}$ probes reveals high levels of expression in olfactory sensory neurons (Figure 2Ab). In contrast, no hybridization is observed in mutant animals homozygous for the $G_{olf}$ deficiency (Figure 2Ag). The RNA probe used in these hybridization experiments includes the entire $G_{olf}$ coding region, suggesting that the mutant allele expresses no $G_{olf}$ RNA despite the fact that we have deleted only the first four exons. Control in situ hybridizations with two other components of the presumed olfactory signal transduction cascade, the CNG channel (Figures 2Ad and 2Ai), and adenylate cyclase type III (Figures 2Ae and 2Aj), reveal identical patterns of expression in wild-type and $G_{olf}$ mutants. Moreover, the patterns of expression of the olfactory marker protein (OMP) (Figures 2Aa and 2Af) and the $G_{olf}$ homolog $G_s$ (Figures 2Ac and 2Ah) are indistinguishable in wild-type and $G_{olf}$ mutants.

Immunocytochemistry with antibodies reactive against both $G_{olf}$ and $G_s$ reveals intense staining in the cilia along the axon tracts as well as in the glomeruli in the olfactory bulb of wild-type animals (Figures 2Ba and 2Bc). A significant reduction in $G_{olf}/G_s$ staining is observed in $G_{olf}$ mutant animals, consistent with the observation that $G_{olf}$ is the predominant $G\alpha_s$ subtype in olfactory sensory neurons (Jones, 1990; Figures 2Be and 2Bg). Control immunohistochemistry with an antibody specific for adenylate cyclase type III (Figures 2Bb and 2Bf) reveals identical patterns of expression in both the cell body and cilia of wild-type and mutant animals. Finally, the gross and microscopic anatomy of the olfactory epithelium appears normal in $G_{olf}$ mutant animals (data not shown).

We have also performed in situ hybridization with putative olfactory receptor genes to ask whether the pattern of expression of olfactory receptors is altered in mutant mice. Individual olfactory neurons are thought to express only one of the 1000 receptor genes (Buck, 1992; Chess et al., 1994; C. Dulac, personal communication). Each olfactory receptor is expressed in a small subpopulation of neurons in one of four broad zones in the olfactory epithelium (Ressler et al., 1993; Vassar et al., 1993). The receptor genes *M50*, *P2*, and *M12* are expressed by neurons in zones I, III, and IV, respectively.

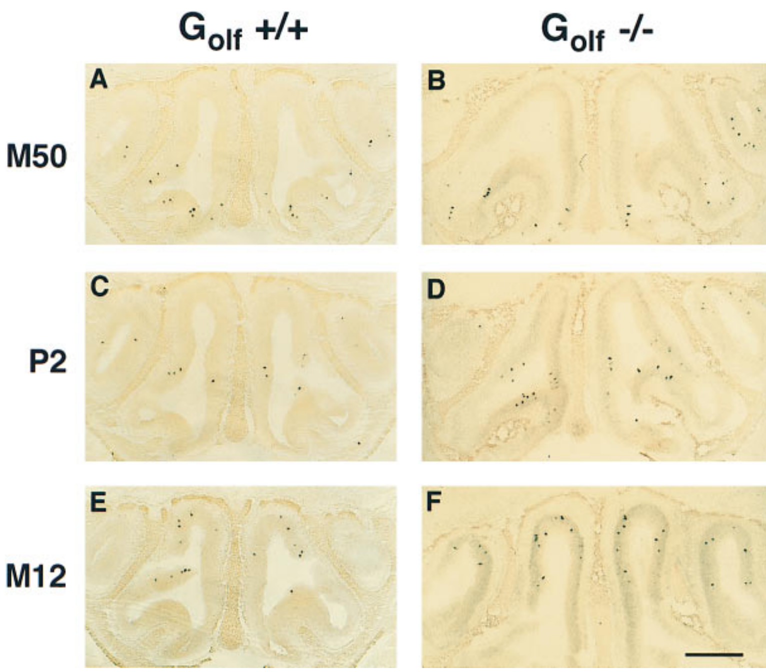


Figure 3. Patterns of Olfactory Receptor Expression in Wild-Type and $G_{olf}$ Mutant Mice

In situ hybridization was performed on 15 μm coronal sections from wild-type ([A], [C], and [E]) and mutant ([B], [D], and [F]) mice ~5 days old. Coronal sections (15 μm) were hybridized with digoxigenin–labeled receptor RNA probes. Alkaline phosphatase–conjugated anti-digoxigenin antibody was used to visualize dark purple positive signals.
(A and B) M50 receptor in zone I.
(C and D) P2 receptor expressed in zone III.
(E and F) M12 receptor expressed in zone IV.
Wild-type and mutant animals reveal little difference in the zonal expression patterns of these receptor genes. Since animals are not littermates, their age may differ by as much as 12 hr, accounting for the variability in number of positive cells. Scale bar, 500 μm.

In situ hybridization with RNA probes for these three receptors reveals a zonal pattern of receptor expression that is essentally indistinguishable in wild-type and $G_{olf}$ mutant animals (Figure 3). Taken together, these data demonstrate that the organization of the olfactory sensory epithelium and the expression of a set of olfactory-specific genes thought to be involved in olfactory signal transduction are not likely to be perturbed in $G_{olf}$ mutant animals.

### Odor-Evoked Response Is Deficient in $G_{olf}$ Mutants

We next characterized the electrophysiological response to odors in wild-type and $G_{olf}$ mutant mice. In order to discern whether odor-evoked potentials are mediated by $G_{olf}$, we performed electro-olfactogram (EOG) recordings that measure the extracellular field potential elicited by odors across a local area of sensory cells in the olfactory epithelium (Figure 4). This field potential is generated by the extracellular current resulting from the inward current across the ciliary membrane and the outward current across the ciliary and somatic membranes (Ottoson, 1956; Takagi et al., 1968; Lowe and Gold, 1991). The EOG recordings from wild-type neonatal mice demonstrate that each of seven structurally distinct odors elicits a transient negative potential with maximal responses of 4 mV (Figure 4A). In neonatal $G_{olf}$ mutants, the magnitude of the EOG response observed with each of the odors is reduced 70%–80% when compared with wild-type animals (Figure 4A). Moreover, the EOG responses in $G_{olf}$ mutants are markedly slowed and prolonged, suggesting an impairment in adaptation. The wild-type and mutant responses reach peak amplitude to odors at about 0.7 and 1.5 s, respectively, after the initiation of the response. Since adaptation in olfactory receptor cells is mediated by $Ca^{2+}$ influx that results in desensitization of the cyclic nucleotide–gated channel (Kurahashi and Shibuya, 1990; Kurahashi and Menini, 1997), the prolonged response kinetics suggest that the small currents in the $G_{olf}$ mutant mice do not allow sufficient $Ca^{2+}$ entry to desensitize the channel.

The reduction in EOG response is even more pronounced in mutant animals that survive beyond 3 weeks (Figure 4B). In these older animals, the amplitude of the EOG is <2.5% of that observed for wild-type mice. In addition, the response latency in $G_{olf}$-deficient mice relative to wild-type littermates increases from 36 ms at P1 to 49 ms at P21 (Figure 4C). Similar differences in the EOG response are independent of the position of the electrode. One odor, triethylamine, elicits a rapidly rising positive potential that is observed in mutant mice. A similar response is apparent with this odor in mice deficient in the CNG channel (Brunet et al., 1996). This positive response is thought to reflect an odor-evoked secretory mechanism in nonneuronal support cells, which is typically masked in wild-type EOGs by the negative neuronal component (Okano and Takagi, 1974).

It is possible that the diminution in the amplitude of the EOG in response to odors in mutant mice does not reflect the direct involvement of $G_{olf}$ in an odor-evoked signal transduction cascade. The absence of $G_{olf}$, for example, may result in nonspecific alterations in the electrophysiological properties of the membrane of sensory neurons. Increases in the resting potential of mutant neurons toward more positive potentials, for example, would diminish odor responsivity independent of whether $G_{olf}$ was directly involved in the odor-evoked signal transduction cascade. Cell-attached patch-clamp recordings performed on individual olfactory neurons in tissue slices, however, reveal that the rate of spontaneous spike generation is similar in mutant and wild-type mice (Figure 4D). Since the threshold for a spike generation lies close to the resting membrane potential, we infer from these data that the resting potential of olfactory sensory cells is similar in mutant and wild-type cells.

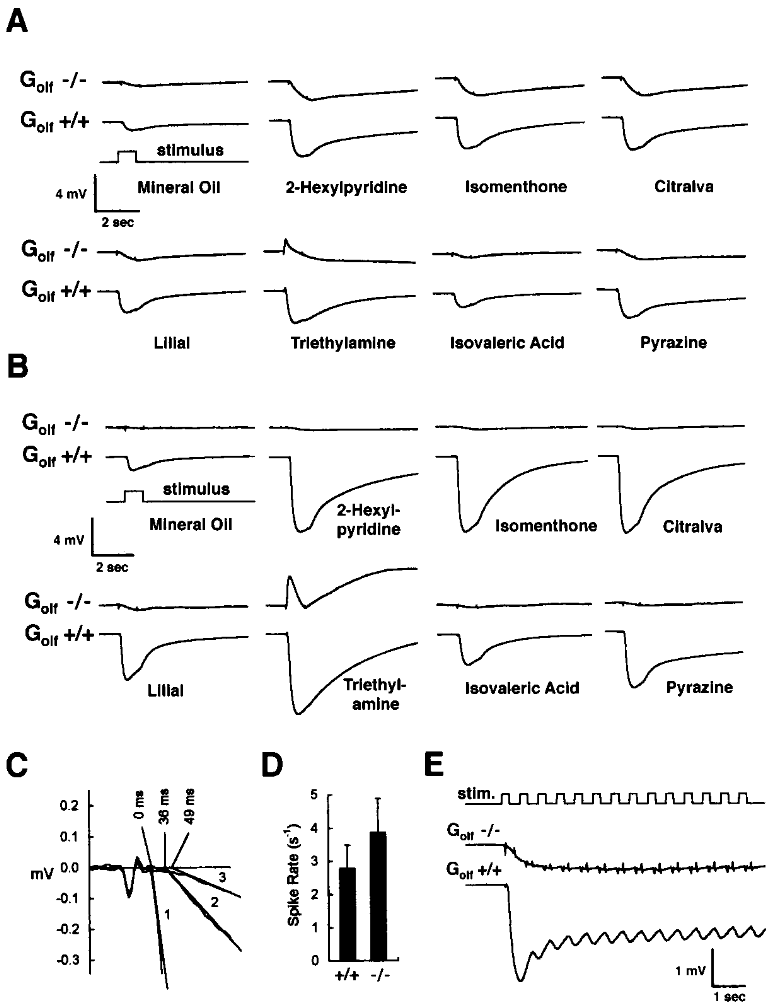


Figure 4. Electro-Olfactogram (EOG) Recordings from Olfactory Epithelium of Wild-Type and $G_{olf}$ Mutant Mice

(A) EOG responses in a newborn wild-type (+/+) and $G_{olf}$ mutant (−/−) littermates. The traces of responses in mutant mice have been plotted at twice the gain of the wild-type trace to make the responses in mutants more readily visible. 2-Hexylpyridine, isomenthone, and citralva elevate cAMP levels (Sklar et al., 1986; Breer and Boekhoff, 1991), whereas lilial, triethylamine, isovaleric acid, and pyrazine elevate $IP_3$ (Boekhoff at al., 1990; Breer and Boekhoff, 1991).

(B) EOG responses in 3-week-old wild-type and $G_{olf}$ mutant littermates. The traces of the mutant have been plotted at four times the gain of wild type to make the responses more readily visible.

(C) Latency of responses in wild-type and $G_{olf}$ mutant mice. Trace 1 is from a newborn wild type, trace 2 is from a newborn mutant, and trace 3 is from a 3-week-old mutant. Latency was defined by fitting the intercept between the baseline and a straight line fitted to the initial slope of the responses. The odorant was 2-hexylpyridine for all three traces.

(D) Comparison between the basal spike rates in newborn wild-type ($n = 4$) and mutant ($n = 3$) mice. The means were not significantly different ($P = 0.4$). Error bars, SEM.

(E) Responses of newborn wild-type and mutant littermates to a train of odorant pulses consisting of 0.2 s odorant followed by 0.3 s odorant off. The trace in mutants is plotted at four times the gain of the wild-type trace to make the response more readily visible. The spikes in the mutant trace are capacitative artifacts that occur upon valve actuation. The odorant was 2-hexylpyridine for both traces.

Moreover, the time course of individual action potentials is the same in $G_{olf}$ mutant and wild-type littermates, suggesting that the voltage-dependent properties of the mutant olfactory neuron membranes are not nonspecifically altered as a consequence of a deficiency in $G_{olf}$.

Most $G_{olf}$ mutant mice fail to suckle, dying within 3 days of birth despite their having measurable EOG data (Figure 4A). If the failure to suckle indeed reflects functional anosmia, this could be a function of the 75% reduction in the peak amplitude of the EOG response observed in newborn mutant animals or a consequence of the slow kinetics of the EOG response observed in $G_{olf}$ mutants (Figure 4C). Recordings from either olfactory bulb or pyriform cortex demonstrate a burst of spikes synchronized with sniffing (Di and Freeman, 1985; Bressler, 1988; Wellis and Scott, 1990; Vanderwolf, 1992). The bursting of postsynaptic cells in synchrony with sniffing is likely to be a consequence of potential fluctuations in the sensory afferents that also coincide with sniffing. If, however, the $G_{olf}$ mutant mice reveal slow response kinetics, it may not be possible for sensory neurons in mutant animals to exhibit fluctuations in the membrane potential at the sniff frequency. To test this hypothesis, we recorded the EOG responses to a train of odor pulses (200 ms of odor followed by 300 ms of clean air) to generate an artificial sniff frequency of 2 Hz (Figure 4E). Responses recorded in wild-type epithelia reveal fluctuations in EOG of 0.28 mV at the 2 Hz sniff frequency, which should result in a burst of spikes in the sensory afferent. In contrast, in $G_{olf}$ mutant mice, there was a slow rise in the EOG response with fluctuations of only 14 $\mu$V at the 2 Hz sniff frequency, a response unlikely to elicit synchronous bursting of sensory neurons. If a burst of spikes is indeed important for the perception of odors, then the slow response kinetics of $G_{olf}$ mutant mice may preclude bursting at the sniff frequency, resulting in functional anosmia. Irrespective of mechanism, these results indicate that $G_{olf}$ plays an essential role in the signaling cascade activated by odors on olfactory sensory neurons, and this deficiency in $G_{olf}$ is likely to result in a functional anosmia.

### Sensory Axon Targeting in $G_{olf}$ Mutant Mice

Neurons expressing a given receptor, although randomly distributed within a given zone in the olfactory epithelium, project their axons to a single medial and a single lateral glomerulus within the olfactory bulb (Ressler et al., 1994a; Vassar et al., 1994; Mombaerts et al., 1996). Moreover, the position of these glomeruli is

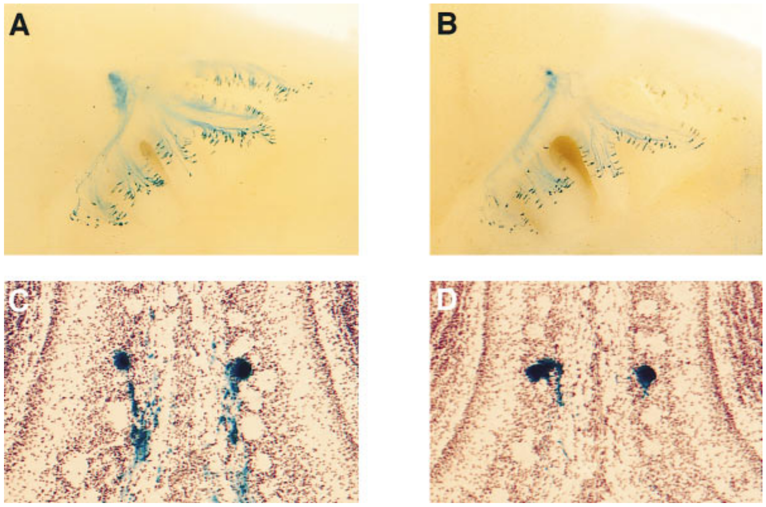


Figure 5. Convergence of P2 Axons in Wild-Type and $G_{olf}$ Mutant Mice

(A and B) Whole-mount view of nasal cavity and the medial aspect of the olfactory bulb in newborn mice. *P2–IRES–tau–lacZ* (+/−) mice either wild-type (A) or mutant (B) for $G_{olf}$ were stained with X-Gal to reveal P2-expressing olfactory neurons in the epithelium and the convergence of P2 axons in the olfactory bulb. Both wild-type and $G_{olf}$ mutant mice reveal convergence of P2 neurons in the bulb. (C and D) Coronal sections (15 μm) of newborn mice through the turbinates and olfactory bulb. *P2–IRES–tau–lacZ* (+/−) mice either wild-type (C) or mutant (D) for $G_{olf}$ stained with X-Gal revealing P2 axons converging upon a single glomerulus in wild-type and mutant littermates.

topographically fixed in all mice examined. Recent experiments suggest that the odorant receptors themselves play an instructive role in guiding axons to their appropriate location within the olfactory bulb (Mombaerts et al., 1996; Wang et al., personal communication). We therefore asked whether the function of the odorant receptors in the guidance process is mediated by $G_{olf}$. The presence of $G_{olf}$ in sensory axons as well as in glomeruli suggests a possible role for $G_{olf}$ in the transduction of guidance information (Figure 2Bc). To this end, we have examined the establishment of a topographic map in homozygous $G_{olf}$-deficient mice. In previous experiments, we developed a genetic approach to visualize axons from specific olfactory neurons as they project to the bulb (Mombaerts et al., 1996). Briefly, we have modified the *P2* receptor gene by targeted mutagenesis in the germline of mice. The *P2* locus now encodes a bicistronic mRNA by virtue of an internal ribosome entry site (IRES) that allows the translation of the P2 receptor, along with tau–lacZ, a fusion of the microtubule-associated protein tau with β-galactosidase. In these strains of mice, olfactory neurons that transcribe the *P2* gene also express tau–lacZ in their axons, permitting the direct visualization of the pattern of projections to the brain (Figure 5). In these genetically altered mice, the dendrites, cell bodies, and axons of P2 neurons exhibit a blue color after staining with X-Gal. The blue axons are readily visualized as they emerge from the epithelium and pass through the cribriform plate to the olfactory bulb, where they converge on a single glomerulus on both the medial and lateral aspect of the olfactory bulb. Moreover, the position of these glomeruli are relatively constant in all mice examined. A similar pattern of P2–IRES–tau–lacZ expression is observed in the olfactory epithelium with convergence of the blue fibers to a topographically fixed locus, when the *P2–IRES–tau–lacZ* allele is crossed into strains bearing the deficiency in $G_{olf}$ (Figure 5). Thus, $G_{olf}$ expression does not appear to be essential for the generation of a precise topographic map in the olfactory bulb.

## $G_{olf}$ Expression in the Brain

Previous studies have demonstrated that $G_{olf}$ is not restricted to olfactory sensory neurons but is expressed in diverse brain regions (Drinnan et al., 1991; Herve et al., 1993). In accord with these studies, we observe high levels of $G_{olf}$ RNA in the basal ganglia, including the caudate, putamen, and nucleus accumbens (Herve et al., 1993; Figure 6A) with lower levels in the globus pallidus and substantia nigra (data not shown). $G_{olf}$ is also highly expressed in the olfactory tubercle, the dentate gyrus, the CA3 region of the hippocampus, and the Purkinje cells of the cerebellum (Figure 6A). Although most brain regions that express $G_{olf}$ also express even higher levels of the homolog $G\alpha_s$, in situ hybridization reveals high levels of $G_{olf}$ expression in the striatum with little or no $G\alpha_s$ detected (Figures 6Ba–6Bh). As expected, no $G_{olf}$ RNA is detectable in the brain by in situ hybridization in homozygous mutant mice (Figures 6Bi–6Bl). Moreover, the levels of $G_s$ RNA are largely unaltered as a consequence of the $G_{olf}$ deficiency (Figures 6Bm–6Bp). In order to discern the function of $G_{olf}$ in these brain regions, we have examined the consequences of $G_{olf}$ mutation on locomotion by measuring the level of motor activity in an open field test in both mutant and wild-type mice. Measurements of mean path length traveled during a 1 hr test session in the light phase demonstrated significant hyperactivity in mutant mice. The mean path length for $G_{olf}$-deficient mice was over 5 times greater than for wild-type mice (Figure 7). Moreover, whereas habituation is observed by 15 min in wild-type mice, no habituation was observed over the 1 hr test period in the mutants (data not shown). These data demonstrate that mice with a homozygous deficiency in $G_{olf}$ exhibit hyperactive behavior. Thus, the expression of $G_{olf}$ in olfactory sensory neurons as well as in discrete brain regions, taken together with the behavior of $G_{olf}$ mutant mice, suggest that $G_{olf}$ may play a central role not only in olfactory signaling events but in signal transduction in the CNS as well.

## Discussion

The initial event in the detection of odors is thought to require the interaction of odor molecules with seven transmembrane receptors on the cilia of olfactory sensory neurons. Our data indicate that the efficient transduction of odor binding into alterations in membrane

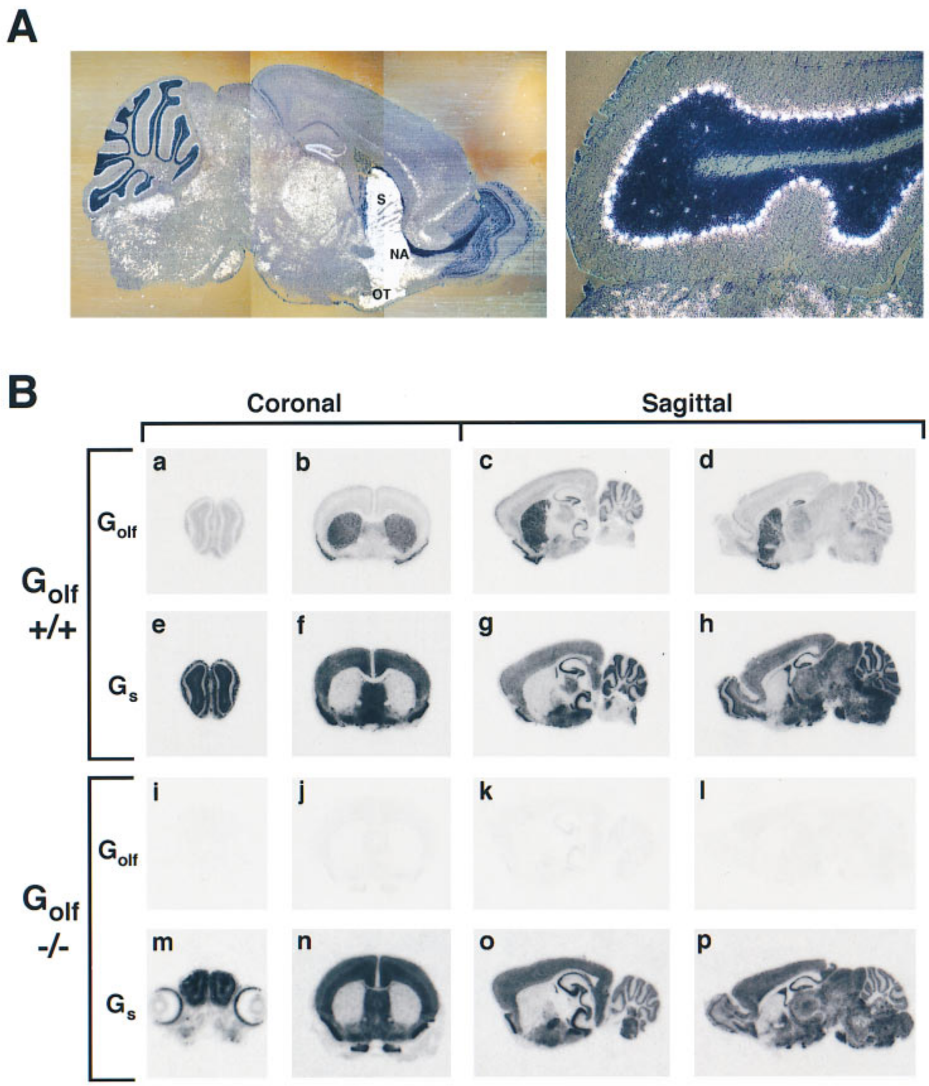


Figure 6. $G_{olf}$ Expression in the Brain

(A) $G_{olf}$ RNA in basal ganglia and cerebellum. In situ hybridization was performed using $^{33}$P-UTP–labeled $G_{olf}$ RNA probes on 15 μm sections from wild-type mice. Panels are photographed in dark field such that white silver grains depict positive signals.

(Left) Sagittal section of adult mouse brain reveals $G_{olf}$ expression in several brain regions, with highest levels in the striatum (S), nucleus accumbens (NA), olfactory tubercle (OT), hippocampus (dentate gyrus and CA3 region), and cerebellum. High levels were also detected in the thalamus, pontine nuclei, and frontal cortex.

(Right) High power view of the cerebellar region in the left panel shows $G_{olf}$ expression in Purkinje cells.

(B) Comparison of RNA expression pattern for $G_{olf}$ and $G_s$ in the brain of wild-type and $G_{olf}$ mutant mice. In situ hybridization was performed using $^{33}$P-UTP–labeled RNA probes on 15 μm sections from 4-week-old wild-type and $G_{olf}$ mutant mice. After hybridization, slides were exposed to Hyperfilm (Amersham), producing dark grains in regions positive for $G_{olf}$ probe.

(a–d) Wild-type mouse brain sections hybridized with $G_{olf}$ probe.

(e–h) Wild-type brain sections hybridized with $G_s$ probe.

(i–l) $G_{olf}$ mutant mice hybridized with $G_{olf}$ probe.

(m–p) $G_{olf}$ mutant mice hybridized with $G_s$ probe.

(a and e) Isolated olfactory bulb.

(a, e, i, and m) Coronal section through anterior head reveals olfactory bulb.

(b, f, j, and n) Coronal section through striatum.

(c, g, k, and o) Lateral sagittal section through brain.

(d, h, l, and p) Medial sagittal section through brain. No hybridization to $G_{olf}$ RNA is detected in $G_{olf}$ mutant mice, whereas $G_s$ expression is largely unaltered.

potential requires the activation of $G_{olf}$ (Figure 4). Activated $G_{olf}$ can then associate with adenylate cyclase, elevating intracellular cAMP, which in turn opens a cyclic nucleotide–gated cation channel. In support of this mechanism, most odors elicit elevations in cAMP (Lowe et al., 1989). Moreover, there is a strong correlation between the extent of cAMP elevation in response to a given odor and the magnitude of the observed EOG response (Lowe et al., 1989). Finally, mice lacking either $G_{olf}$ or the CNG cation channel exhibit dramatic reduc-

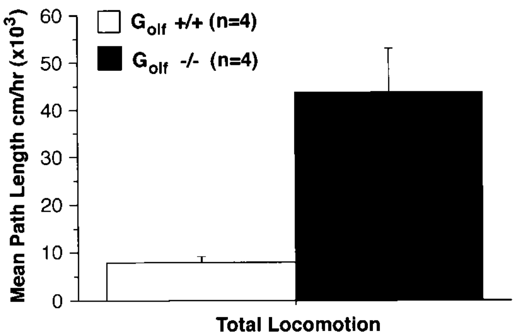


Figure 7. Basal Locomotor Activity in $G_{olf}$ Mutant and Wild-Type Mice

An open field test was conducted on wild-type (white bar) and $G_{olf}$ mutant (black bar) mice. Values represent mean ± SEM path length traveled (cm) in a 1 hr test session during the light phase. Wild-type mice, 8037.88 cm (SEM = 1077.47); $G_{olf}$ mutant mice, 43687.66 cm (SEM = 9104.45). P value = 0.0081.

tions in the electrophysiological response to all odors tested and reveal behavioral phenotypes consistent with the inability to smell (Brunet et al., 1996).

Most $G_{olf}$-deficient mice die from starvation within a few days after birth, due to an inability to suckle. EOG recordings in neonatal $G_{olf}$ mutants reveal a 75% reduction in the magnitude of the response to a wide variety of different odors when compared to heterozygous or wild-type littermates (Figure 4A). EOG recordings on rare survivors at 3 weeks of age show even more profound decreases in response to odors (Figure 4B). One explanation for the increasing severity of this deficiency with age is suggested by the observation that olfactory sensory neurons express both $G_s$ and $G_{olf}$ (Jones et al., 1988; Jones and Reed, 1989). These two proteins share extensive sequence homology, and activation of either protein can elicit elevations in cAMP in cultured cells (Jones et al., 1990). During embryogenesis, the level of $G_s$ in olfactory neurons exceeds that of $G_{olf}$ (Menco et al., 1994). However, early in postnatal development, the $G_{olf}$ level rises and greatly exceeds that of $G_s$ (Jones, 1990). It is therefore possible that in early postnatal mutant mice, odorant receptors couple to $G_s$ and elicit EOG responses, albeit of reduced magnitude. At later times, the level of $G_s$ is dramatically reduced, such that in $G_{olf}$ mutants no odor-evoked EOG response can be observed.

Biochemical and genetic evidence indicate that odor-evoked elevations in cAMP play a significant role in olfactory signal transduction, whereas the role of odor-elicited increases in inositol 1,4,5-trisphosphate ($IP_3$) in vertebrate olfactory processing is far less clear. The observation that those odors that do not elevate cAMP levels in isolated cilia often result in increases in $IP_3$ has led to the suggestion that different classes of odors activate distinct second-messenger systems in olfactory sensory neurons (Anholt and Rivers, 1990; Breer, 1993; Ache and Zhainazarov, 1995; Restrepo et al., 1996). Mice mutant for either $G_{olf}$ or the CNG channel exhibit striking reductions in the EOG response to all odors tested, including those odors shown to elevate intracellular $IP_3$ levels (Brunet et al., 1996). These data suggest that if an elevation in $IP_3$ indeed mediates odor-evoked currents, these currents require both the activation of $G_{olf}$ and the CNG channel. Although cAMP-mediated inward currents are readily observed in olfactory cilia, an $IP_3$-gated current has not yet been demonstrated in mammalian olfactory membranes (Firestein et al., 1991; Lowe and Gold, 1993a; Kleene et al., 1994; Nakamura et al., 1996). Moreover, if one subset of odors signals through an $IP_3$-mediated second-messenger pathway and a second subset elevates intracellular cAMP, then $G_{olf}$ must couple to distinct effectors (adenylate cyclase or phospholipase C) in response to different odors.

Evidence for two distinct pathways of signal transduction in two different chemosensory cells has emerged from behavioral genetic experiments in the nematode *C. elegans*. The recognition of volatile chemoattractants in *C. elegans* is accomplished by two pairs of chemosensory cells, AWA and AWC (Bargmann et al., 1993). A single G protein, ODR-3, is thought to couple with the seven transmembrane domain receptors and is required in olfactory neurons that signal through different cation channels (Roayaie et al., 1998 [this issue of *Neuron*]). Chemosensory responses in the AWC neurons require a cyclic nucleotide–gated channel (TAX-2 and TAX-4), whereas chemoattraction mediated by AWA neurons requires a structurally distinct cation channel (OSM-9) (Coburn and Bargmann, 1996; Colbert et al., 1997). It is not yet clear whether these two distinct channels are activated by different second messengers, but a single G protein, ODR-3, is capable of regulating different ion channels in different neurons, each eliciting a similar behavioral response to odors (Roayaie et al., 1998).

## The Establishment of the Topographic Map

The precise pattern of projections of olfactory sensory neurons in the olfactory bulb provides a topographic map of receptor activation that defines the quality of a sensory stimulus. Recent genetic experiments, along with in situ hybridization analysis of receptor mRNA in the bulb, demonstrate that neurons expressing a given receptor, and therefore responsive to a given odor, project with precision to two of the 1800 glomeruli within the mouse olfactory bulb (Ressler et al., 1994a; Vassar et al., 1994; Mombaerts et al., 1996). Since the position of individual glomeruli is topographically defined, the bulb provides a spatial map that identifies which of the numerous receptors have been activated. Thus, the quality of an olfactory stimulus is encoded by different patterns of spatial activity within the bulb (Stewart et al., 1979; Lancet et al., 1982; Kauer et al., 1987; Imamura et al., 1992; Mori et al., 1992; Katoh et al., 1993; Friedrich and Korsching, 1997; Joerges et al., 1997). These observations pose an interesting but complex problem in axon guidance.

How do neurons expressing a given receptor know which target to project to in the bulb? In one model, the odorant receptor itself could recognize a set of guidance cues expressed by bulbar cells. In this manner, an olfactory neuron would be afforded a distinct identity that dictates the nature of the odor to which it responds as well as the glomerular target to which its axons project.

Support for such a model derives from recent genetic experiments in which we have examined the pattern of projection of neurons that bear deletions in the receptor genes but nonetheless express the reporter molecule, tau–lacZ, allowing us to visualize the pattern of projections in the olfactory bulb (Wang et al., personal communication). In these animals, convergence is no longer observed; rather, individual neurons appear to wander in the outer nerve layer. Second, we have performed a series of receptor-swap experiments in which the coding sequence of the *P2* receptor was substituted with that of other odorant receptors (Mombaerts et al., 1996; Wang et al., personal communication). In each instance, we observe that the receptor swap alters the patterns of projection, suggesting that the olfactory receptor plays an instructive role in the guidance process but cannot be the sole determinant in axon targeting. Such a model suggests that the odorant receptor will be expressed on dendrites where it recognizes odors in the environment and also on axon termini where it would recognize a set of guidance cues.

Analysis of the electrophysiological properties of olfactory sensory neurons in $G_{olf}$ mutant mice strongly suggests that odorant receptors on the dendrites couple with $G_{olf}$ to translate the binding of odors into alterations in membrane potential (Figure 4). If receptors do serve as guidance receptors on axon termini, and $G_{olf}$ protein is present in the glomeruli (Figure 2Bc), it is reasonable to ask whether this function of odorant receptors also requires the activation of $G_{olf}$. To this end, we have examined the pattern of projections in neurons expressing the P2 odorant receptor in $G_{olf}$ mutants and their wild-type littermates. Convergence of P2 axons to two of the 1800 glomeruli is observed in both wild-type and mutant mice (Figure 5). These observations suggest that the signal transduction pathway activated by receptors to guide axonal projections does not employ $G_{olf}$ and therefore differs from the pathway that translates the recognition of odors into neural activity in the dendrite. One candidate molecule, $G_s$, could couple with receptors on axon termini, since high levels of $G_s$ are present in olfactory neurons at developmental times when the topographic map is generated (Menco et al., 1994).

Convergence of the P2 fibers in newborn $G_{olf}$ mutant mice is observed despite a significant reduction in odor-evoked potentials in the sensory epithelium. This observation is consistent with independent experiments that demonstrate the establishment of a precise topographic map in mice lacking the olfactory CNG ion channel (L. Brunet, F. Wang, R.A., and J. Ngai, unpublished data). CNG mutant mice fail to exhibit odor-evoked electrophysical responses in the sensory epithelium, but the pattern of convergence of like axons in the bulb is unaltered in these mutant mice. Taken together, these data argue that olfactory experience is not required for the establishment or the refinement of the topographic map but do not exclude a role for activity-dependent processes in the maintenance or potential plasticity of the map after it is established.

## The Behavioral Phenotype of $G_{olf}$-Deficient Mice

Analysis of $G_{olf}$ expression by either in situ hybridization or immunocytochemistry reveals that $G_{olf}$ is not only expressed in olfactory sensory neurons but is also expressed in several other neural and nonneural tissues (Jones and Reed, 1989; Herve et al., 1993; Zigman et al., 1993; Figure 6). High levels of $G_{olf}$ RNA are expressed in the striatum, notably in the caudate, putamen, and nucleus accumbens, with lower levels in the substantia nigra and globus pallidus. $G_{olf}$ is also abundant in CA3 and the dentate gyrus of the hippocampus. Finally, $G_{olf}$ RNA and protein expression is observed in a mosaic pattern in developing spermatocytes within the testis (Parmentier et al., 1992; Zigman et al., 1993).

The behavioral phenotype and electrophysiological properties of olfactory sensory neurons in $G_{olf}$ mutants argue strongly for a central role of $G_{olf}$ in olfactory signal transduction, coupling odor binding with elevations in cAMP. $G_{olf}$ mutant mice are unable to feed at birth, and rare surviving females exhibit deficient mothering behaviors. Both suckling and nurturing are thought to be olfactory-driven behaviors mediated by the main olfactory system (Teicher et al., 1980; Calamandrei et al., 1992; Mayer and Rosenblatt, 1993; Coppola et al., 1994; Romeyer et al., 1994; Levy et al., 1991; Griffith and Williams, 1996; Brunet et al., 1996). Consistent with these olfactory behavioral deficits, $G_{olf}$ mutant mice exhibit dramatically reduced EOG responses to all odors examined. The rare homozygotes that do survive to sexual maturity are fertile and mate, a finding consistent with experiments that indicate that mating behaviors depend on pheromone recognition by the vomeronasal sensory neurons (that do not express $G_{olf}$), rather than the main olfactory system (Rajendren et al., 1990; Meredith and Fernandez, 1994; Meek et al., 1994). We cannot, however, exclude the possibility that the behavioral phenotypes we observe result from the deficiency of $G_{olf}$ in CNS neurons. Deletion of $G_{olf}$ specifically in olfactory sensory neurons would be required definitively to attribute these behavioral defects to deficits in olfactory sensory neurons. In addition, since $G_{olf}$ mutants were derived from a single ES cell colony, it remains possible that the phenotypes observed are the consequence of mutations in ES cells at loci other than $G_{olf}$. Sufficient backcrossing, which would allow us to exclude this possibility, has not yet been performed.

Finally, open-field testing reveals that surviving $G_{olf}$-deficient animals exhibit hyperactive behaviors. By 8 weeks of age, $G_{olf}$ mutants exhibit over five times the locomotor activity of wild-type animals. A locomotor phenotype is not surprising in $G_{olf}$ mutant mice, since $G_{olf}$ is expressed at high levels in the striatum and cerebellum, brain regions essential in regulating and coordinating movements. Within the basal ganglia, dopaminergic fibers originating in the substantia nigra innervate the caudate and putamen, and this neural pathway is essential to regulate movement (Marshall and Berrios, 1979; Altar and Marshall, 1988; Marshall and Joyce, 1988; Hauber, 1996). A second set of dopaminergic fibers innervate the nucleus accumbens (mesolimbic system), and this pathway has been implicated in the regulation of motivated behaviors (Koob, 1996; Salamone, 1996; Robbins and Everitt, 1996). D1- and D2-like dopamine receptors are expressed on the targets of these striationigral pathways. The D1-like receptors activate adenylate cyclase, presumably by coupling to a $G\alpha_s$-like subunit (Monsma et al., 1990). In situ hybridizations and immunohistochemistry indicate that neurons expressing dopamine D1-like receptors in the striatum are likely to express high levels of $G_{olf}$ and relatively little $G_s$ (Herve et al., 1993, 1995). These data suggest that the $G_{olf}$ mutant mice will exhibit severely compromised dopamine D1-like activity in these brain regions. Pharmacological experiments support a complex network of interactions between D1-like and D2-like receptors in the striatum, such that the two receptors synergize to regulate locomotor activity (Keefe and Gerfen, 1995; Gerfen et al., 1995). However, in one study, mice homozygous for a dopamine D1 receptor deficiency exhibit hyperactive behaviors in locomotor assays (Xu et al., 1994), a phenotype in accord with the hyperactive behaviors we observed in $G_{olf}$ mutants (Figure 7). It should be noted that the observation that $G_{olf}$ and D1 receptor mutants enhance motor activity is inconsistent with pharmacological experiments that suggest that activation of the dopamine D1 systems enhance movement (Zebrowska et al., 1977; Shiosaki et al., 1996). Thus, our data suggest that $G_{olf}$ may function in more diverse brain regions than was previously appreciated and that $G_{olf}$ mutant mice may ultimately contribute to our understanding of the complex neural pathways by which the various dopamine receptors interact to coordinate movement.

## Experimental Procedures

### Generation of a Targeted Mutation in $G_{olf}$

A cDNA encoding the rat $G_{olf}$ gene was used to isolate a mouse P1 plasmid encoding the mouse $G_{olf}$ gene from a P1 library of mouse genomic DNA. A 6.2 XbaI-NdeI fragment was isolated from the P1 plasmid that contained the first four exons of the $G_{olf}$ gene. PCR was used to introduce PacI linkers within the first exon immediately upstream of the ATG and immediately downstream of exon 4. PacI digestion therefore removes a 1.65 fragment containing the coding region of the first four exons of the $G_{olf}$ gene. This region was replaced with a 1.7 kb *pgk-neo* cassette (Adra et al., 1987) flanked by PacI sites, such that transcription of *pgk-neo* was n the opposite orientation from $G_{olf}$. This targeting vector contains 0.83 kb of $G_{olf}$ homologous sequence at the 5′ end and 3.7 kb at the 3′ end (Figure 1).

The construct was electroporated into 129/Sv ES cells and screened for positive $neo^r$ colonies using G418, as described (Mombaerts et al., 1996). Colonies were picked, and their genomic DNA was digested with HindIII and hybridized with a 3′ $G_{olf}$ probe (Figure 1). Southern blot analysis revealed a single homologous recombinant from 396 $neo^r$ colonies. This clone was expanded and used to generate chimeras by microinjection into blastocysts derived from C57Bl/6 females. The mice were in a mixed (129 X C57Bl/6) background. The mutation was transmitted through the germline, and both male and female heterozygotes showed no abnormal phenotype. Mutants were derived from crossing F1 heterozygotes. The F1 mice result from the mating of 129 germline chimera with C57Bl/6 mice producing heterozygous $G_{olf}$ mutant offspring. Crossing of F1 heterozygotes produced homozygous mutant pups at the expected frequency of 25% and were indistinguishable from wild-type and heterozygous littermates at birth. By P3, 70% of the homozygous mutants died. Rare survivors were smaller than heterozygous and homozygous littermates, and this difference was apparent by 1 week of age (see Results). At 1 week, we trimmed the litter to enhance survival of the mutants by removing most of the wild-type and heterozygous pups in order to reduce competition, while allowing a few to remain with the homozygous mutants to aid with milk flow and production by the mother.

### $G_{olf}$/*P2–IRES–tau–lacZ* Mutant Mice

*P2–IRES–tau–lacZ* mutant mice were generated as described (Mombaerts et al., 1996). In these mice, *IRES–tau–lacZ* sequences were introduced 3′ to the *P2* gene, such that receptor function was not disturbed and cells expressing the modified *P2* allele also expressed *tau–lacZ*. F1 mice heterozygous for the $G_{olf}$ mutation were crossed with homozygous *P2–IRES–tau–lacZ* mutant mice, generating F2 compound heterozygotes, which were crossed to one another to generate mice homozygous for the $G_{olf}$ mutation and either heterozygous or homozygous for the *P2–IRES–tau–lacZ* allele.

### In Situ Hybridizations

In situ hybridization was carried out on 20 μM fresh frozen sections with either $^{33}$P-UTP– or digoxigenin-UTP–labeled riboprobes. cDNA clones encoding OMP (Buiakova et al., 1994), $G_{olf}$ (Jones and Reed, 1989), $G_s$ (Sullivan et al., 1986), CNG (Dhallan et al., 1990), adenylate cyclase type III (Bakalyar and Reed, 1990), and the odorant receptors M50 (Ressler et al., 1994b), P2, and M12 (Mombaerts et al., 1996) were obtained by RT-PCR. Under the in situ hybridization conditions employed, the $G_{olf}$ and $G_s$ probes did not cross-hybridize. In situ hybridizations using digoxigenin-UTP– (Schaeren and Gerfin, 1993) and $^{33}$P-UTP– (Wilkinson et al., 1987) labeled probes were performed as previously described (Vassar et al., 1993, 1994).

### Immunohistochemistry

Immunohistochemistry was performed on 5-day-old mice. Heads were fresh frozen in OCT (Miles), and 20 μM coronal sections were cut and mounted. Slides were then fixed in 4% paraformaldehyde, washed in PTw (PBS + 0.1% Tween-20) and blocked with PTw + 10% HINGS (heat-inactivated goat serum, Gibco). Tissue was then reacted with rabbit polyclonal antibodies specific for adenylate cyclase type III or $G_{olf}$/$G_s$(Santa Cruz Biotechnology) at a 1:500 dilution. The bound primary antibody was then visualized using Cy2–conjugated anti-rabbit IgG (Jackson Laboratories).

### Electrophysiology

Odorant stimulation and EOG recordings were carried out as described (Brunet et al., 1996). Mice were sacrificed by decapitation and EOG recordings were performed on the medial surface of the olfactory turbinates. Genotyping was performed on tails of sacrificed animals by Southern blotting. Odorant concentrations are expressed as the concentration of odor in the liquid phase contained within the evaporation tubes. Recording signals were low-pass filtered at 30 Hz and digitized at 125 Hz. Cell–attached patch-clamp recordings (Hamill et al., 1981) were performed on individual olfactory neurons in tissue slices using solutions as described (Lowe and Gold, 1993b). Recordings were low-pass filtered at 2 kHz and digitized at 8 kHz.

### X-Gal Staining

For whole mounts, tissues were fixed for 30 min on ice with 100 mM phosphate buffer (pH 7.4), 4% paraformaldehyde, 2 mM $MgSO_4$, and 5 mM EGTA. Samples were washed at room temperature with buffer A (100 mM phosphate buffer [pH 7.4], 2 mM $MgCl_2$, and 5 mM EGTA), once for 5 min and then once for 30 min, followed by two washes of 5 min at room temperature with buffer B (100 mM phosphate buffer [pH 7.4], 2 mM $MgCl_2$, 0.01% sodium desoxycholate, and 0.02% Nonidet P40). The blue precipitate was generated by exposure in the dark at 37°C to buffer C (buffer B with 5 mM potassium-ferricyanide, 5 mM potassium-ferrocyanide, and 0.5 mg/ml of X-Gal). Tissues fresh frozen in OCT (Miles) were sectioned at a thickness of 15–20 μm, fixed, and stained with X-Gal as above. Sections were then counterstained with hematoxylin (Sigma), dehydrated, and mounted with Accu-mount 60 (Baxter).

### Locomotor Activity

Open-field testing was conducted during the hours of 0800 and 1700. Animals were placed in square chambers (20 $cm^2$) and monitored throughout the 1 hr test session by a video tracking system (PolyTrack, San Diego, CA) that recorded the animals' locations and paths. Data regarding each animal's path length was collected and summed for each 5 min interval during the test session. These successive measurements were totaled and analyzed using StatView 4.5 (Abacus Concepts) statistical software.

**Acknowledgments**

We thank Fan Wang for advice, Kimberly Scearce and Rene Hen for performing the locomotor assay, Monica Mendelsohn for technical assistance, Cori Bargmann for sharing data prior to publication, Tom Jessell and members of the Axel lab for critically reviewing the manuscript, and Phyllis Kisloff for preparation of the manuscript. This work was supported by the Howard Hughes Medical Institute and by a grant from the National Institutes of Health, NCI 5PO1 CA23767 (R.A.).

Received October 28, 1997; revised December 9, 1997.

**References**

Ache, B.W., and Zhainazarov, A. (1995). Dual second-messenger pathways in olfactory transduction. Curr. Opin. Neurobiol. *5*, 461–466.

Adra, C.N., Boer, P.H., and McBurney, M.W. (1987). Cloning and expression of the mouse pgk-1 gene and the nucleotide sequence of its promoter. Gene *60*, 65–74.

Altar, C.A., and Marshall, J.F. (1988). Neostriatal dopamine uptake and reversal of age-related movement disorders with dopamine-uptake inhibitors. Ann. NY Acad. Sci. *515*, 343–354.

Anholt, R.R., and Rivers, A.M. (1990). Olfactory transduction: cross-talk between second-messenger systems. Biochemistry *29*, 4049–4054.

Bakalyar, H.A., and Reed, R.R. (1990). Identification of a specialized adenylyl cyclase that may mediate odorant detection. Science *250*, 1403–1406.

Bargmann, C.I., Hartwieg, E., and Horvitz, H.R. (1993). Odorant-selective genes and neurons mediate olfaction in C. elegans. Cell *74*, 515–527.

Ben-Arie, A.N., Lancet, D., Taylor, C., Khen, M., Walker, N., Ledbetter, D.H., Carrozzo, R., Patel, K., Sheer, D., Lehrach, H., et al. (1994). Olfactory receptor gene cluster on human chromosome 17: possible duplication of an ancestral receptor repertoire. Hum. Mol. Genet. *3*, 229–235.

Boekhoff, I., Tareilus, E., Strottmann, J., and Breer, H. (1990). Rapid activation of alternative second messenger pathways in olfactory cilia from rats by different odorants. EMBO J. *9*, 2453–2458.

Breer, H. (1993). Second messenger signalling in olfaction. Ciba Found. Symp. *179*, 97–109.

Breer, H., and Boekhoff, I. (1991). Odorants of the same odor class activate different second messenger pathways. Chem. Senses *16*, 19–29.

Breer, H., Boekhoff, I., and Tareilus, E. (1990). Rapid kinetics of second messenger formation in olfactory transduction. Nature *345*, 65–68.

Bressler, S.L. (1988). Changes in electrical activity of rabbit olfactory bulb and cortex to conditioned odor stimulation. Behav. Neurosci. *102*, 740–747.

Brunet, L.J., Gold, G.H., and Ngai, J. (1996). General anosmia caused by a targeted disruption of the mouse olfactory cyclic nucleotide–gated cation channel. Neuron *17*, 681–693.

Buck, L.B. (1992). The olfactory multigene family. Curr. Opin. Genet. Dev. *2*, 467–473.

Buck, L., and Axel, R. (1991). A novel multigene family may encode odorant receptors: a molecular basis for odor recognition. Cell *65*, 175–187.

Buiakova, O.I., Krishna, N.S., Getchell, T.V., and Margolis, F.L. (1994). Human and rodent OMP genes: conservation of structural and regulatory motifs and cellular localization. Genomics *20*, 452–462.

Calamandrei, G., Wilkinson, L.S., and Keverne, E.B. (1992). Olfactory recognition of infants in laboratory mice: role of noradrenergic mechanisms. Physiol. Behav. *52*, 901–907.

Chess, A., Simon, I., Cedar, H., and Axel, R. (1994). Allelic inactivation regulates olfactory receptor gene expression. Cell *78*, 823–834.

Coburn, C.M., and Bargmann, C.I. (1996). A putative cyclic nucleotide–gated channel is required for sensory development and function in C. elegans. Neuron *17*, 695–706.

Colbert, H.A., Smith, T.L., and Bargmann, C.I. (1997). OSM-9, a novel protein with structural similarity to channels is required for olfaction, mechanosensation, and olfactory adaptation in Caenorhabditis elegans. J. Neurosci. *17*, 8259–8269.

Conklin, B.R., Herzmark, P., Ishida, S., Voyno, Y.T., Sun, Y., Farfel, Z., and Bourne, H.R. (1996). Carboxyl-terminal mutations of Gq alpha and Gs alpha that alter the fidelity of receptor activation. Mol. Pharmacol. *50*, 885–890.

Coppola, D.M., Coltrane, J.A., and Arsov, I. (1994). Retronasal or internasal olfaction can mediate odor-guided behaviors in newborn mice. Physiol. Behav. *56*, 729–736.

Dhallan, R.S., Yau, K.W., Schrader, K.A., and Reed, R.R. (1990). Primary structure and functional expression of a cyclic nucleotide activated channel from olfactory neurons. Nature *347*, 184–187.

Di, P.G., and Freeman, W.J. (1985). Odor-related bulbar EEG spatial pattern analysis during appetitive conditioning in rabbits. Behav. Neurosci. *99*, 964–978.

Drinnan, S.L., Hope, B.T., Snutch, T.P., and Vincent, S.R. (1991). Golf in the basal ganglia. Mol. Cell Neurosci. *2*, 66–70.

Firestein, S., and Werblin, F. (1989). Odor-induced membrane currents in vertebrate-olfactory receptor neurons. Science *244*, 79–82.

Firestein, S., Darrow, B., and Shepherd, G.M. (1991). Activation of the sensory current in salamander olfactory receptor neurons depends on a G protein-mediated cAMP second messenger system. Neuron *6*, 825–835.

Friedrich, R.W., and Korsching, S.I. (1997). Combinatorial and chemotopic odorant coding in the zebrafish olfactory bulb visualized by optical imaging. Neuron *18*, 737–752.

Frings, S., and Lindemann, B. (1991). Current recording from the sensory cilia of olfactory receptor cells in situ. I. The neuronal response to cyclic nucleotides. J. Gen. Physiol. *97*, 1–16.

Gerfen, C.R., Keefe, K.A., and Gauda, E.B. (1995). D1 and D2 dopamine receptor function in the striatum: coactivation of D1- and D2-dopamine receptors on separate populations of neurons results in potentiated immediate early gene response in D1-containing neurons. J. Neurosci. *15*, 8167–8176.

Griffith, M.K., and Williams, G.L. (1996). Roles of maternal vision and olfaction in suckling-mediated inhibition of luteinizing hormone secretion, expression of maternal selectivity, and lactational performance of beef cows. Biol. Reprod. *54*, 761–768.

Hamill, O.P., Marty, A., Neher, E., Sakmann, B., and Sigworth, F.J. (1981). Improved patch-clamp techniques for high-resolution current recording from cells and cell-free membrane patches. Pflügers Arch. *391*, 85–100.

Hauber, W. (1996). Impairments of movement initiation and execution induced by a blockade of dopamine D1 or D2 receptors are reversed by a blockade of N-methyl-D-aspartate receptors. Neuroscience *73*, 121–130.

Herve, D., Levi, S.M., Marey, S.I., Verney, C., Tassin, J.P., Glowinski, J., and Girault, J.A. (1993). G(olf) and Gs in rat basal ganglia: possible involvement of G(olf) in the coupling of dopamine D1 receptor with adenylyl cyclase. J. Neurosci. *13*, 2237–2248.

Herve, D., Rogard, M., and Levi, S.M. (1995). Molecular analysis of the multiple Golf alpha subunit mRNAs in the rat brain. Brain Res. Mol. Brain Res. *32*, 125–134.

Imamura, K., Mataga, N., and Mori, K. (1992). Coding of odor molecules by mitral/tufted cells in rabbit olfactory bulb. I. Aliphatic compounds. J. Neurophysiol. *68*, 1986–2002.

Joerges, J., Kuttner, A., Galizia., G, and Menzel, R. (1997). Representations of odours and odour mixtures visualized in the honeybee brain. Nature *387*, 285–288.

Jones, D.T. (1990). Distribution of the stimulatory GTP-binding proteins, Gs and Golf, within olfactory epithelium. Chem. Senses *15*, 333–340.

Jones, D.T., and Reed, R.R. (1987). Molecular cloning of five GTP-binding protein cDNA species from rat olfactory neuroepithelium. J. Biol. Chem. *262*, 14241–14249.

Jones, D.T., and Reed, R.R. (1989). Golf: an olfactory neuron specific-G protein involved in odorant signal transduction. Science *244*, 790–795.

Jones, D.T., Barbosa, E., and Reed, R.R. (1988). Expression of G-protein alpha subunits in rat olfactory neuroepithelium: candidates for olfactory signal transduction. Cold Spring Harb. Symp. Quant. Biol. *1*, 349–353.

Jones, D.T., Masters, S.B., Bourne, H.R., and Reed, R.R. (1990). Biochemical characterization of three stimulatory GTP-binding proteins. The large and small forms of Gs and the olfactory-specific G-protein, Golf. J. Biol. Chem. *265*, 2671–2676.

Katoh, K., Koshimoto, H., Tani, A., and Mori, K. (1993). Coding of odor molecules by mitral/tufted cells in rabbit olfactory bulb. II. Aromatic compounds. J. Neurophysiol. *70*, 2161–2175.

Kauer, J.S., Senseman, D.M., and Cohen, L.B. (1987). Odor-elicited activity monitored simultaneously from 124 regions of the salamander olfactory bulb using a voltage-sensitive dye. Brain. Res. *418*, 255–261.

Keefe, K.A., and Gerfen, C.R. (1995). D1-D2 dopamine receptor synergy in striatum: effects of intrastriatal infusions of dopamine agonists and antagonists on immediate early gene expression. Neuroscience *66*, 903–913.

Kleene, S.J., Gesteland, R.C., and Bryant, S.H. (1994). An electrophysiological survey of frog olfactory cilia. J. Exp. Biol. *195*, 307–328.

Koob, G.F. (1996). Hedonic valence, dopamine and motivation. Mol. Psychiatry *1*, 186–189.

Kurahashi, T. (1989). Activation by odorants of cation-selective conductance in the olfactory receptor cell isolated from the newt [published erratum appears in J. Physiol. (Lond.) *424*, 561–562]. J. Physiol. (Lond.) *419*, 177–192.

Kurahashi, T. and Shibuya, T. (1990). $Ca^{2+}$-dependent adaptive properties in the solitary olfactory receptor cell of the newt. Brain Res. *515*, 261–268.

Kurahashi, T., and Menini, A. (1997). Mechanism of odorant adaptation in the olfactory receptor cell [see comments]. Nature *385*, 725–729.

Lancet, D., Greer, C.A., Kauer, J.S., and Shepherd, G.M. (1982). Mapping of odor-related neuronal activity in the olfactory bulb by high-resolution 2-deoxyglucose autoradiography. Proc. Natl. Acad. Sci. USA *79*, 670–674.

Levy, N.S., Bakalyar, H.A., and Reed, R.R. (1991). Signal transduction in olfactory neurons. J. Steroid Biochem. Mol. Biol. *39*, 633–637.

Lowe, G., and Gold, G.H. (1991). The spatial distributions of odorant sensitivity and odorant-induced currents in salamander olfactory receptor cells. J. Physiol. (Lond.) *442*, 147–168.

Lowe, G., and Gold, G.H. (1993a). Contribution of the ciliary cyclic nucleotide–gated conductance to olfactory transduction in the salamander. J. Physiol. (Lond.) *462*, 175–196.

Lowe, G., and Gold, G.H. (1993b). Nonlinear amplification by calcium-dependent chloride channels in olfactory receptor cells. Nature *366*, 283–286.

Lowe, G., Nakamura, T., and Gold, G.H. (1989). Adenylate cyclase mediates olfactory transduction for a wide variety of odorants. Proc. Natl. Acad. Sci. USA *86*, 5641–5645.

Marshall, J.F., and Berrios, N. (1979). Movement disorders of aged rats: reversal by dopamine receptor stimulation. Science *206*, 477–479.

Marshall, J.F., and Joyce, J.N. (1988). Basal ganglia dopamine receptor autoradiography and age-related movement disorders. Ann. NY Acad. Sci. *515*, 215–225.

Masters, S.B., Stroud, R.M., and Bourne, H.R. (1986). Family of G protein alpha chains: amphipathic analysis and predicted structure of functional domains. Protein Eng. *1*, 47–54.

Masters, S.B., Landis, C.A., and Bourne, H.R. (1990). Mutational analysis of the structure and function of GTP-binding proteins. Adv. Enzyme. Regul. *30*, 75–87.

Mayer, A.D., and Rosenblatt, J.S. (1993). Contributions of olfaction to maternal aggression in laboratory rats (Rattus norvegicus): effects of peripheral deafferentation of the primary olfactory system. J. Comp. Psychol. *107*, 12–24.

Meek, L.R., Lee, T.M., Rogers, E.A., and Hernandez, R.G. (1994). Effect of vomeronasal organ removal on behavioral estrus and mating latency in female meadow voles (Microtus pennsylvanicus). Biol. Reprod. *51*, 400–404.

Menco, B.P., Tekula, F.D., Farbman, A.I., and Danho, W. (1994). Developmental expression of G-proteins and adenylyl cyclase in peripheral olfactory systems. Light microscopic and freeze-substitution electron microscopic immunocytochemistry. J. Neurocytol. *23*, 708–727.

Meredith, M., and Fernandez, F.G. (1994). Vomeronasal system, LHRH, and sex behaviour. Psychoneuroendocrinology *19*, 657–672.

Miller, R.T., Masters, S.B., Sullivan, K.A., Beiderman, B., and Bourne, H.R. (1988). A mutation that prevents GTP-dependent activation of the alpha chain of Gs. Nature *334*, 712–715.

Mombaerts, P., Wang, F., Dulac, C., Chao, S.K., Nemes, A., Mendelsohn, M., Edmondson, J., and Axel, R. (1996). Visualizing an olfactory sensory map. Cell *87*, 675–686.

Monsma, F.J., Mahan, L.C., McVittie, L.D., Gerfen, C.R., and Sibley, D.R. (1990). Molecular cloning and expression of a D1 dopamine receptor linked to adenylyl cyclase activation. Proc. Natl. Acad. Sci. USA *87*, 6723–6727.

Mori, K., Mataga, N., and Imamura, K. (1992). Differential specificities of single mitral cells in rabbit olfactory bulb for a homologous series of fatty acid odor molecules. J. Neurophysiol. *67*, 786–789.

Nakamura, T., and Gold, G.H. (1987). A cyclic nucleotide–gated conductance in olfactory receptor cilia. Nature *325*, 442–444.

Nakamura, T., Lee, H.H., Kobayashi, H., and Satoh, T.O. (1996). Gated conductances in native and reconstituted membranes from frog olfactory cilia. Biophys. J. *70*, 813–817.

Okano, M., and Takagi, S.F. (1974). Secretion and electrogenesis of the supporting cell in the olfactory epithelium. J. Physiol. (Lond.) *242*, 353–370.

Ottoson, D. (1956). Analysis of the electrical activity of the olfactory epithelium. Acta Physiol. Scand. *35* (suppl.), 1–83.

Pace, U., Hanski, E., Salomon, Y., and Lancet, D. (1985). Odorant-sensitive adenylate cyclase may mediate olfactory reception. Nature *316*, 255–258.

Parmentier, M., Libert, F., Schurmans, S., Schiffmann, S., Lefort, A., Eggerickx, D., Ledent, C., Mollereau, C., Gerard, C., Perret, J., et al. (1992). Expression of members of the putative olfactory receptor gene family in mammalian germ cells. Nature *355*, 453–455.

Rajendren, G., Dudley, C.A., and Moss, R.L. (1990). Role of the vomeronasal organ in the male-induced enhancement of sexual receptivity in female rats. Neuroendocrinology *52*, 368–372.

Ressler, K.J., Sullivan, S.L., and Buck, L.B. (1993). A zonal organization of odorant receptor gene expression in the olfactory epithelium. Cell *73*, 597–609.

Ressler, K.J., Sullivan, S.L., and Buck, L.B. (1994a). Information coding in the olfactory system: evidence for a stereotyped and highly organized epitope map in the olfactory bulb. Cell *79*, 1245–1255.

Ressler, K.J., Sullivan, S.L., and Buck, L.B. (1994b). A molecular dissection of spatial patterning in the olfactory system. Curr. Opin. Neurobiol. *4*, 588–596.

Restrepo, D., Teeter, J.H., and Schild, D. (1996). Second messenger signaling in olfactory transduction. J. Neurobiol. *30*, 37–48.

Roayaie, K., Crump, J.C., Sagasti, A., and Bargmann, C.I. (1998). The G$\alpha$ protein ODR-3 mediates olfactory and nociceptive function and controls cilium morphogenesis in *C. elegans* olfactory neurons. Neuron *20*, this issue, 55–67.

Robbins, T.W., and Everitt, B.J. (1996). Neurobehavioural mechanisms of reward and motivation. Curr. Opin. Neurobiol. *6*, 228–236.

Romeyer, A., Poindron, P., and Orgeur, P. (1994). Olfaction mediates the establishment of selective bonding in goats. Physiol. Behav. *56*, 693–700.

Salamone, J.D. (1996). The behavioral neurochemistry of motivation: methodological and conceptual issues in studies of the dynamic activity of nucleus accumbens dopamine. J. Neurosci. Methods *64*, 137–149.

Schaeren, W.N., and Gerfin, M.A. (1993). A single protocol to detect transcripts of various types and expression levels in neural tissue and cultured cells: in situ hybridization using digoxigenin-labelled cRNA probes. Histochemistry *100*, 431–440.

Shiosaki, K., Asin, K.E., Britton, D.R., Giardina, W.J., Bednarz, L., Mahan, L., Mikusa, J., Nikkel, A., and Wismer, C. (1996). Hyperactivity and behavioral seizures in rodents following treatment with the dopamine D1 receptor agonists A-86929 and ABT-431. Eur. J. Pharmacol. *317*, 183–190.

Sklar, P.B., Anholt, R.R., and Snyder, S.H. (1986). The odorant-sensitive adenylate cyclase of olfactory receptor cells. Differential stimulation by distinct classes of odorants. J. Biol. Chem. *261*, 15538–15543.

Stewart, W.B., Kauer, J.S., and Shepherd, G.M. (1979). Functional organization of rat olfactory bulb analysed by the 2-deoxyglucose method. J. Comp. Neurol. *185*, 715–734.

Sullivan, K.A., Liao, Y.C., Alborzi, A., Beiderman, B., Chang, F.H., Masters, S.B., Levinson, A.D., and Bourne, H.R. (1986). Inhibitory and stimulatory G proteins of adenylate cyclase: cDNA and amino acid sequences of the alpha chains. Proc. Natl. Acad. Sci. USA *83*, 6687–6691.

Takagi, S.F., Wyse, G.A., Kitamura, H., and Ito, K. (1968). The role of sodium and potassium ions in the generation of the electro-olfactogram. J. Gen. Physiol. *51,* 552–578.

Teicher, M.H., Stewart, W.B., Kauer, J.S., and Shepherd, G.M. (1980). Suckling pheromone stimulation of a modified glomerular region in the developing rat olfactory bulb revealed by the 2-deoxyglucose method. Brain Res. *194*, 530–535.

Vanderwolf, C.H. (1992). Hippocampal activity, olfaction, and sniffing: an olfactory input to the dentate gyrus. Brain Res. *593*, 197–208.

Vassar, R., Ngai, J., and Axel, R. (1993). Spatial segregation of odorant receptor expression in the mammalian olfactory epithelium. Cell *74*, 309–318.

Vassar, R., Chao, S.K., Sitcheran, R., Nunez, J.M., Vosshall, L.B., and Axel, R. (1994). Topographic organization of sensory projections to the olfactory bulb. Cell *79*, 981–991.

Wellis, D.P., and Scott, J.W. (1990). Intracellular responses of identified rat olfactory bulb interneurons to electrical and odor stimulation. J. Neurophysiol. *64*, 932–947.

Wilkinson, D.G., Bailes, J.A., Champion, J.E., and McMahon, A.P. (1987). A molecular analysis of mouse development from 8–10 days *post-coitum* detects changes only in eukaryotic globin expression. Development *99*, 493–500.

Xu, M., Moratalla, R., Gold, L.H., Hiroi, N., Koob, G.F., Graybiel, A.M., and Tonegawa, S. (1994). Dopamine D1 receptor mutant mice are deficient in striatal expression of dynorphin and in dopamine-mediated behavioral responses. Cell *79*, 729–742.

Zebrowska, L.I., Przegalinski, E., Sloniec, M., and Kleinrok, Z. (1977). Clonidine-induced locomotor hyperactivity in rats. The role of central postsynaptic alpha-adrenoceptors. Naunyn Schmiedebergs Arch. Pharmacol. *297*, 227–231.

Zigman, J.M., Westermark, G.T., LaMendola, J., Boel, E., and Steiner, D.F. (1993). Human G(olf) alpha: complementary deoxyribonucleic acid structure and expression in pancreatic islets and other tissues outside the olfactory neuroepithelium and central system. Endocrinology *133*, 2508–2514.